



Synthesis, characterization and DNA interaction of a novel Pt(II) macrocyclic Schiff base complex containing the piperazine moiety and its cytotoxicity and molecular docking

Leila Nemati^a, Hassan Keypour^{a,*}, Nahid Shahabadi^b, Saba Hadidi^b, Robert William Gable^c

^a Faculty of Chemistry, Bu-Ali Sina University, Hamedan 65174, Iran

^b Inorganic Chemistry Department, Faculty of Chemistry, Razi University, Kermanshah, Iran

^c School of Chemistry, University of Melbourne, Victoria 3010, Australia

ARTICLE INFO

Article history:

Received 22 January 2021

Revised 12 April 2021

Accepted 21 April 2021

Available online 24 April 2021

Keywords:

Piperazine moiety

Schiff base

Pt(II) complex

DNA interaction

Partial intercalation

Cytotoxicity

Molecular docking

ABSTRACT

A new platinum Schiff base complex, $[C_{17}H_{28}N_4OPt]Cl_2$ (1) was prepared from the condensation of a poly-amine containing piperazine moiety, (1,4-bis(3-aminopropyl)piperazine) and 2-hydroxy-benzaldehyde (H_2L), in the presence of Pt^{2+} ion and examined by mass, FT-IR, elemental analysis 1H NMR and ^{13}C NMR. The structure of the metal complex has been confirmed by a single-crystal X-ray structural analysis in which the Pt atom is in a square planar coordination environment. The crystal was found to be composed of two complexes that co-crystallized, the formulation being $0.973[C_{17}H_{28}N_4OPt]Cl_2$, $0.014[[C_{17}H_{27}N_4OPt]_2PtCl_2]Cl_2$. The ligand and Schiff base complex interactions with calf thymus DNA (ct-DNA) were studied using UV-Vis and fluorescence spectroscopy and molecular docking simulations. UV-Vis absorption investigations indicated hypochromism and hyperchromism effects, respectively, for the ligand and the complex. The binding constant of the Pt(II) complex with DNA ($6.1 \times 10^4 M^{-1}$) was greater than the corresponding binding value of the ligand ($4 \times 10^3 M^{-1}$). Competitive fluorescence results showed that molecular replacement of Hoechst in the minor groove of DNA by the ligand and Pt(II) complex resulted in the fluorescence of the DNA-Hoechst system being extinguished. Fluorescence emission spectra, using methylene blue (MB) as an intercalate probe, demonstrated only the replacement of MB by the Pt(II) complex from the MB-DNA system. Thermodynamic studies confirmed that van der Waals forces and hydrogen bonds play critical roles in the compounds-DNA binding. Based on the viscosity measurements, the effect of the ligand on DNA viscosity was less than that of the Pt(II) complex. The experimental results were supported by molecular docking studies. The results showed that the Pt(II) complex interacts with DNA via a partial intercalation mode, while the free ligand showed binding to DNA in the minor groove. In vitro cell, culture studies confirmed that the Pt(II) complex has a remarkable cytotoxic effect on human prostate carcinoma cells.

© 2021 Elsevier B.V. All rights reserved.

1. Introduction

The study of complexes of transition metals and biomolecules (i.e., proteins and DNA) has played a significant role in the development of therapeutic drugs and an understanding of biochemical processes [1,2]. DNA has been the target of anticancer drugs, as its interaction with a molecule may result in damage to the DNA and the subsequent death of the cancer cell. DNA interactions with molecules can occur through both non-covalent and covalent modes, i.e., intercalation and the effects of external static electronic and groove binding [3,4]. Platinum compounds have proven to be

effective chemotherapeutic agents in the treatment of cancer, and so a great deal of research has been carried out with the aim of developing alternatives with improved properties over the standard drug, cisplatin (*cis*-diamminedichloroplatinum(II) - *cis*-DDP) [5,6], by the modification of the ligand set around the platinum atom. Recently, we have witnessed a great deal of interest in synthesizing platinum(II) complexes containing O and N-donors, amines and, especially, Schiff bases complexes [7,8]. These complexes have shown high biological activity, as well as reduced toxicity [9]. Macrocyclic and macrocyclic Schiff-base complexes of transition metal ions have been of great significance in the development of coordination chemistry, [10–13]. Furthermore, they also have been used in catalytic reactions and have been found to have antibacterial, antitumor, antifungal, anticancer [14,15], antimalarial [16],

* Corresponding author.

E-mail address: haskey1@yahoo.com (H. Keypour).

and antioxidant [17] activities. Schiff base complexes containing salicylaldehyde play a significant role in generating metal complexes due to their potential in forming intermolecular hydrogen bonds between the N and the O atoms [18]. The combination of salicylaldehyde with a number of amines in different ratios (1:1 and 2:1) can result in the formation of various bi-, tri-, and tetradentate Schiff base ligands [19,20]. Platinum(II) Schiff base complexes have been evaluated as anticancer agents against prostate, breast, liver, and lung cancer cell lines and have shown considerable cytotoxicity comparable to that of cisplatin [21]. Accordingly, a number of complexes of macrocyclic Schiff-base containing either the homopiperazine or the piperazine moiety have been prepared and evaluated [22–30]. The piperazine moiety can be regarded as a suitable structural building block for the construction of both macrocyclic and macroacyclic compounds, due to the presence of hydrogen-bond acceptors, terminal amino protons, and great ability to form metal ion complexes [31,32]. As part of continuing research aiming at obtaining more effective anticancer drugs, with fewer side effects, we report the synthesis of a new platinum(II) complex with macrocycle containing the piperazine moiety, $[C_{17}H_{28}N_4OPt]Cl_2$ (1).

2. Experimental

2.1. Materials

Potassium tetrachloroplatinat(II), 1,4-bis(3-aminopropyl)piperazine, salicylaldehyde, methylene blue, DMSO, methanol, and ethanol were supplied from Merck. The ct-DNA, Tris-HCl, Hoechst 33258, were obtained from Sigma Co and applied without further purification. Deionized water was applied to prepare the buffer.

2.2. Physical measurements

Spectra of 1H and ^{13}C NMR were recorded in DMSO d_6 on a spectrometer of Bruker Advance 400 MHz using the internal standard of $Si(CH_3)_4$. CHN analyses have been performed on a Perkin-Elmer (2400 series 2) CHNS/O elemental analyzer. The mass spectrometer of Agilent technologies (HP) 5973, operating at a potential of ionization of 70 eV to record mass spectra, has been applied.

KBr pellets were used to record infrared spectra on a spectrometer of BIO-RADFTS-40A at a wavelength between 4000 and 400 cm^{-1} .

2.3. Sample preparation

Experiments were carried out in a buffer solution containing Tris-HCl, double distilled water, and hydrogen chloride at pH 7.4. The ligand and its Pt(II) complex were dissolved in a solvent mixture of 5% ethanol and 95% Tris-HCl buffer at room temperature. The UV absorption at 260 nm and 280 nm of the ct-DNA solution showed an absorbance ratio of 1.8–1.9, indicating that the DNA was protein naked [33,34]. The ct-DNA concentration was determined from the intensity of the absorption at 260 nm using a molar extinction coefficient of 6600 $M^{-1} cm^{-1}$ [35].

2.4. UV-Vis spectroscopy studies

Absorbance spectra were obtained by a spectrophotometer (Nordantec T80). The concentration of DNA was changed between (0 to 1.67×10^{-3} M, ligand; 0 to 5.9×10^{-4} M, Pt(II) complex) and compounds concentration was fixed (2.43×10^{-5} M, ligand; 1.5×10^{-4} M, Pt(II) complex) at during the absorbance measurements. The spectra were measured in the range 200–300 nm for the ligand and 300–500 nm for the Pt(II) complex.

2.5. Competitive fluorescence

Competitive fluorescence experiments were measured using a JASCO spectrofluorometer (FP 6200). The aqueous solutions of methylene blue and Hoechst 33,258 (1×10^{-3} M) were used to investigate the competitive ability of ligand and Pt(II) complex for DNA binding sites. The fluorescence experiments were carried out at three different temperatures (288, 298, and 310 K).

2.6. Viscosity measurements

Viscosity analysis was preformed using a SCHOT AVS 450 viscometer placed in a constant temperature bath (25°C). A digital stopwatch was employed to measure the flow time at a constant DNA concentration (5×10^{-5} M). The viscosity (η) was determined from the mean value of three measurements. Results have been plotted as $(\eta/\eta_0)^{1/3}$ against the [compounds]/[DNA] ratio. In this model, η_0 and η refer to the relative viscosity contributions of DNA in the absence and the presence of the ligand and the Pt(II) complex.

2.7. Molecular docking studies

In order to carry out the blind docking calculations, MGL tools 1.5.4 with Auto Dock 4 and Auto Grid 4 [36,37] were used to carry out the calculations between the ligand and Pt(II) complex with the relevant DNA sequence. The Protein Data Bank was the center to download the DNA sequenced (CGCGAATTCGCG)2 dodecamer (PDB ID: 1BNA). Auto Dock Tools were used to prepare the files of the ligand, the Pt(II) complex and the receptor (DNA). A box was used to enclose the DNA with a grid spacing of 0.375 Å and points of the grid in $x \times y \times z$ directions, $64 \times 78 \times 124$. In this regard, 14.78, 20.976, and 8.807 Å were set as the center of the grid. For each docking simulation, the number of independent docking runs was set to 100. Cluster analysis was performed on the docking results with the application of a tolerance of a root mean square (RMS) of about 0.5 Å. The reference structure was the atomic coordinates of the ligand. HyperChem (Hypercube Inc., Gainesville, FL) was applied to optimize the structure of the molecules. The output from Auto Dock was presented by PyMol [38].

2.8. Cell culture conditions

PC3 (human prostate cell carcinoma), Hela (human cervix cell carcinoma), and cell lines of A431 (human skin cell carcinoma) were obtained from the Iranian Pasteur Institute, Tehran, Iran. Bovine serum, DMEM-F12, penicillin, and streptomycin 3-(4,5-dimethylthiazol-2-yl)-2,5-diphenyl-tetrazolium bromide (MTT) were prepared from Sigma-Aldrich. Cells were cultured in DMEM-F12 (Dulbecco's Modified Eagle's Medium) completed with 10% (V/V) heat 100 IU/mL penicillin, inactivated fetal bovine serum, and 100 $\mu L/mL$ streptomycin and then maintained in a humidified atmosphere (90%) containing 5% CO_2 at 37 °C. The complex was dissolved in DMSO and stored as stock solutions (the concentration of DMSO was < 1%). A medium that contained 0.1% DMSO was used to keep control cells [39].

2.8.1. Cytotoxic assays

The MTT method was applied to evaluate the cytotoxic effects of the Pt(II) complex. Cell lines growing in 96-well plates were treated with various concentrations (0–50 $\mu g/mL$) of the complex. After 24 h treatment, the medium was replaced by 0.5 mg/mL of MTT (100 μL), and the plates were again placed in the incubator (37 °C) for 3–4 h. DMSO (100 ml) was added to dissolve the purple formazan crystals. A microplate reader (Biotech Instruments, USA)

was then used to calculate the optical density (OD570). The IC50 value was computed by plotting the percent cell viability (log10) versus the concentration of each sample. All MTT experiments were performed in triplicate.

2.9. Synthesis

2.9.1. Synthesis of ligand (H₂L)

The ligand (H₂L) was synthesized by modified version of the literature method [40] (Scheme 1). Yield: 0.2 g (90%). Anal. Calc. for C₂₄H₃₂N₄O₂ (MW: 408.3): C, 70.5; H, 7.8; N, 13.7. Found: C, 70.2; H, 7.6; N, 13.9%. EI-MS (*m/z*): 408.3. IR (KBr, cm⁻¹): 1634 ν (C = N), 3429 ν (O–H). ¹H NMR (DMSO *d*₆, ppm) δ_{H} = 1.74–1.76 (4H_h), 2.29–2.32 (4H_i), 2.48 (s, 8H_{j, k}), 3.57 (4H_g), 6.82–7.40 (m, 8H_{b–e}), 8.51 (s, 2H_f), 13.62 (s, 2H(OH)). ¹³C NMR (DMSO *d*₆, ppm) δ_{C} = 27.96 (C_h), 53.26 (C_g), 55.77 (C_i), 56.72 (C_{j, k}), 116.97 (C_d), 118.77 (C_b), 119 (C_i), 131.98 (C_e), 132.63 (C_c), 161.40 (C_m), 166.28 (C_f).

2.9.2. Synthesis of platinum(II) complex

DMSO (3 mmol, 0.24 g) was added to a solution of K₂[PtCl₄] (0.5 mmol, 0.2 g) dissolved in water (3 ml) [41]. The resulting mixture was stirred for 24 h at 25 °C in the dark. A yellow solution was obtained and, then, an ethanolic solution (20 ml) of the ligand H₂L (0.5 mmol, 0.2 g) was increased to this solution. The reaction mixture was stirred for 24 h at 25 °C. The obtained yellow solution remained at room temperature for three days in order to eliminate the remaining DMSO solvent. After washing by diethyl ether and drying in a vacuum, the yellow powder as a pure compound was obtained (Scheme 2). When diethyl ether vapor was slowly diffused into the MeOH solution, the crystalline compound was acquired (Yield: 70%). Anal. Calc. for [C₁₇H₂₈N₄OPt]Cl₂ (MW: 572.83): C, 35.61; H, 4.89; N, 9.78 Found: C, 36.2; H, 5.01; N, 9.31%. EI-MS (*m/z*): 498.3. IR (KBr, cm⁻¹): 1615 ν (C = N), 3411 ν (O–H).

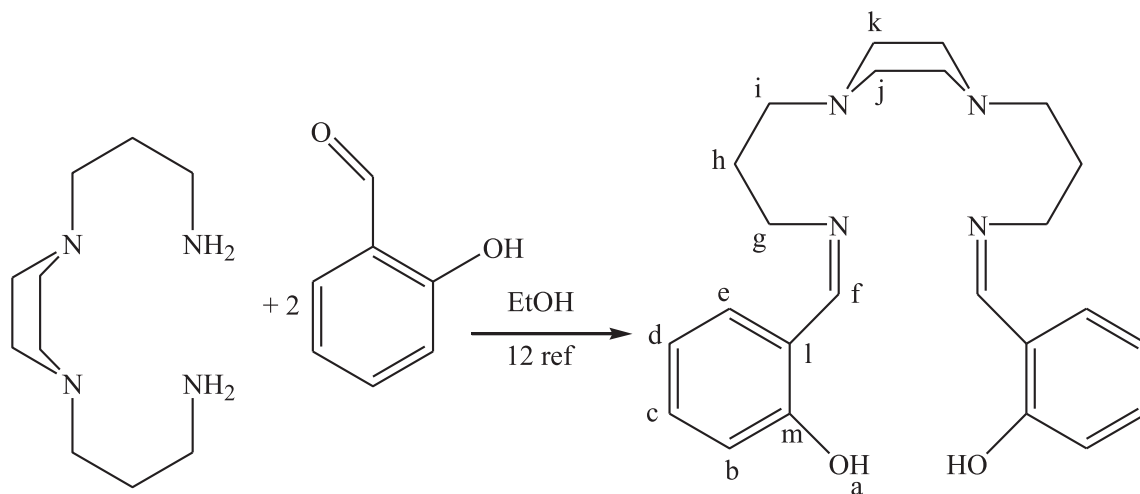
2.9.3. X-ray crystal structure determination

Slow evaporation from methanol was used to crystallize light-yellow single crystals of the complex. Data were collected on a Rigaku Oxford Diffraction Supernova diffractometer using mirror monochromated Mo K α radiation (λ = 0.71073 Å) at 100 K. When applying Olex2 [42], the ShelXT [43] structure solution program helped to solve the structure using Intrinsic Phasing, and Least Squares minimization on F² was used to refine the ShelXL [44] refinement package, using all data. Subsequently, gaussian absorp-

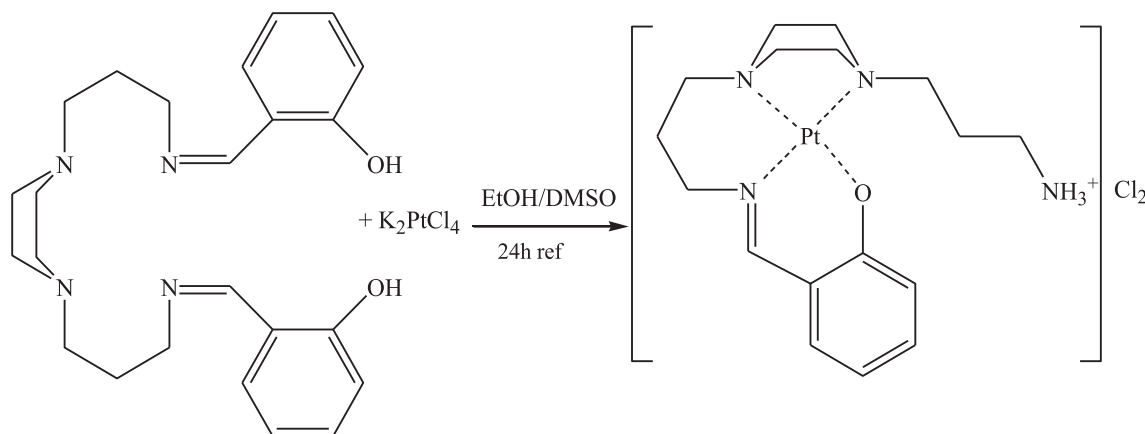
tion reformations were applied to the data [45]. Anisotropic displacement parameters were used to refine the non-hydrogen atoms, while the riding model was used to refine the hydrogen atoms they were incorporated at geometrical estimates. After refining the structure as [C₁₇H₂₈N₄OPt]Cl₂, there was an electron density peak of 3.6 e Å⁻³ lying on a center of symmetry approximately 2 Å from two chloride ions and two nitrogen atoms, in a square planar environment. This was interpreted as partially occupied Pt, a minor contribution from the co-crystallized trinuclear species [C₁₇H₂₇N₄OPt]₂PtCl₄ (2). It was possible to refine both structures, with the components of each atom, apart from the additional Pt atom (Pt2), constrained to have the same coordinates and the same displacement parameters. Moreover, the hydrogen atoms for both components of N4 (–NH₃⁺ for [C₁₇H₂₈N₄OPt]Cl₂ and –NH₂ for [C₁₇H₂₇N₄OPt]₂PtCl₄) were included. The final contribution of [C₁₇H₂₇N₄OPt]₂PtCl₄ to the final structure was 0.0136 (5); the crystal is thus formulated as 0.973[C₁₇H₂₈N₄OPt]Cl₂ · 0.014[[C₁₇H₂₇N₄OPt]₂PtCl₄]. Other crystals from the same batch showed similar additional amounts of Pt (as [C₁₇H₂₇N₄OPt]₂PtCl₄). The final difference map showed a maximum electron density peak of 1.8 e Å⁻³ close to the Pt1 atom; presumably, due to inaccuracies in the absorption corrections or some slight disorder. Table 1 shows the crystallographic data for the platinum complex.

3. Results and discussion

The Schiff base macrocyclic ligand (H₂L) was prepared from the condensation reaction between salicylaldehyde and 1,4-bis(3-aminopropyl) piperazine, in ethanol solution. The platinum complex, [C₁₇H₂₈N₄OPt]Cl₂ (1), was synthesized with the reaction of the metal salt and ligand (H₂L). The mass spectra of the ligand (H₂L) and the Pt(II) complex are shown in Fig. 1A and B, respectively. The ligand (H₂L) spectrum shows a molecular ion peak at 408.3 *m/z*, consistent with the molecular formula C₂₄H₃₂N₄O₂, while the spectrum of the platinum complex shows a molecular ion peak of 498.3 *m/z*, attributed to the [C₁₇H₂₈N₄OPt]²⁺ cation. These results are consistent with the formation of a 1:1 complex between the platinum salt and the ligand (H₂L). A strong peak at 1634 cm⁻¹ in the infrared spectrum of the ligand, attributable to the imine group (ν (C = N) vibration), and the absence of bands characteristic of the starting materials (amine and carbonyl groups) confirms the production of the Schiff base ligand. In the IR spectra of the complex, this band is shifted to become a sharp band at 1614 cm⁻¹, indicative of coordination of the imine nitrogen



Scheme 1. The process for the synthesis of macrocyclic ligand H₂L.



Scheme 2. The process for the synthesis of $[\text{Pt}(\text{H}_2\text{L})]\text{Cl}_2$ complex.

Table 1

Crystal data and structure refinement for $0.973[\text{C}_{17}\text{H}_{28}\text{N}_4\text{OPt}]\text{Cl}_2 \cdot 0.014[\text{C}_{17}\text{H}_{27}\text{N}_4\text{-OPt}]_2\text{PtCl}_2] \text{Cl}_2$.

Empirical formula	$\text{C}_{17}\text{H}_{27.973}\text{Cl}_2\text{N}_4\text{OPt}_{1.014}$
Formula weight	572.83
Temperature/K	100.00(10)
Crystal system	monoclinic
Space group	$\text{P2}_1/\text{n}$
a/Å	9.7970(3)
b/Å	10.5984(3)
c/Å	19.0285(5)
$\alpha/^\circ$	90
$\beta/^\circ$	97.258(3)
$\gamma/^\circ$	90
Volume/Å ³	1959.94(9)
Z	4
$\rho_{\text{calc}}/\text{cm}^{-3}$	1.941
μ/mm^{-1}	7.534
F(000)	1116.0
Crystal size/mm ³	$0.524 \times 0.16 \times 0.152$
Radiation	$\text{Mo K}\alpha$ ($\lambda = 0.71073$)
2θ range for data collection/ $^\circ$	5.688 to 64.922
Index ranges	$-13 \leq h \leq 14, -10 \leq k \leq 15, -28 \leq l \leq 26$
Reflections collected	17,046
Independent reflections	6408 [$R_{\text{int}} = 0.0263, R_{\text{sigma}} = 0.0320$]
Data/restraints/parameters	6408/0/234
Goodness-of-fit on F^2	1.053
Final R indexes [$I > 2\sigma(I)$]	$R_1 = 0.0231, wR_2 = 0.0517$
Final R indexes [all data]	$R_1 = 0.0278, wR_2 = 0.0536$
Largest diff. peak/hole / $e \text{ \AA}^{-3}$	1.83/-1.41

to the metal [46]. The presence of a band at 3411 cm^{-1} , for the Pt (II) complex, is assigned to $\nu(\text{NH}_2)$, indicates partial hydrolysis of the synthesized ligand to form the mono Schiff base ligand, giving rise to a ligand with a N_3O donor set.

3.1. X-ray structural analysis of the platinum(II) complex

$[\text{C}_{17}\text{H}_{28}\text{N}_4\text{OPt}]\text{Cl}_2$ (1): The platinum atom is in a square planar environment, coordinated by both N atoms of the piperazine group, the imine N, and the phenol O (Fig. 2). The Pt-N bond lengths involving the piperazine ring of are longer than the Pt-O and Pt-N bond lengths of the 2-aminomethylphenol group. The 2-aminomethylphenol group is planar and is oriented at 16.34 (9°) to the N_4 plane with the Pt atom lying $0.3741(19)$ Å out of the plane. The aminopropyl group adopts an extended conformation, lying essentially along the $\text{N}2 \dots \text{N}3$ direction; all atoms apart from the terminal nitrogen atom (C15, C16, C17) are coplanar with the PtN_4 plane. The terminal nitrogen of the aminopropyl group, N4, is protonated to give a $-\text{NH}_3^+$ unit with the ligand adopting a

zwitterionic form, giving a $[\text{C}_{17}\text{H}_{28}\text{N}_4\text{OPt}]^{2+}$ cation. Both chloride anions are hydrogen bonding to the terminal amine, the hydrogen bonds involving Cl2 lead to a hydrogen-bonded dimer (Fig. 3). Additional C-H...Cl1 interactions lead to a 3D hydrogen-bonded network.

$[\text{C}_{17}\text{H}_{27}\text{N}_4\text{OPt}]_2\text{PtCl}_2$ (2): Pt2A is in a *trans*- N_2Cl_2 square planar coordination environment arising from two Cl anions and two neutral NH_2 groups, one from each of two $[\text{C}_{17}\text{H}_{27}\text{N}_4\text{OPt}]^+$ cations; the two Pt-N bonds link two $[\text{C}_{17}\text{H}_{27}\text{N}_4\text{OPt}]^+$ cations into a trinuclear structure (Fig. 4). Due to the Pt2A atom lying on a center of symmetry, the PtN_2Cl_2 moiety is planar, with C2-Pt-N angles close to 90° (Table 2). The *trans*- N_2Cl_2 coordination environment is similar to that observed for *trans*-bis(*t*-Butylamine)-dichloro-platinum [47]. Presumably, the hydrogen bonding between the chloride anions and terminal amine atoms, as can be seen from Fig. 2, facilitates the incorporation of any excess Pt in solution, most likely arising from some decomposition of the complex during crystallization. As this component is present in only minor amounts, the possible presence of this in the freshly prepared material would have no impact on any of the other results.

3.2. DNA interaction studies

3.2.1. UV-vis spectroscopy

UV-Vis spectroscopy is a fundamental technique used in DNA binding studies as interactions between DNA and target molecules can result in changes in both the position and intensity of absorbance bands. The two important spectral features arising from changes in the structure of the DNA double helix are hyperchromism (increase in absorbance) and hypochromism (reduction in absorbance). If the binding mode of the DNA with the target molecule is intercalation, groove or is electrostatic then hypochromism results, with intercalation there is usually a red-shift, while hyperchromism occurs when there is structural damage to the double helix of DNA [48–50].

In this study, absorption titration experiments were carried out to evaluate the interaction of ct-DNA with both the ligand and the Pt(II) complex. In these experiments, the concentration of the complex (1.5×10^{-4} M) and ligand (2.43×10^{-5} M) were kept constant. Upon addition of different amounts of DNA (0 to 1.67×10^{-3} M) and (0 to 5.9×10^{-4} M) to the ligand and complex, respectively, an increase in the absorption intensity of the ligand (hyperchromic) (Fig. 5A) and a decrease in the absorption intensity of the complex (hypochromic) with red-shift about 4 nm (376 to 380 nm) were observed (Fig. 5B). The absorption bands below 670 nm in the spectrum of the Pt(II) complex are consistent with the Pt(II) being in a low-spin d^8 square-planar environment [51].

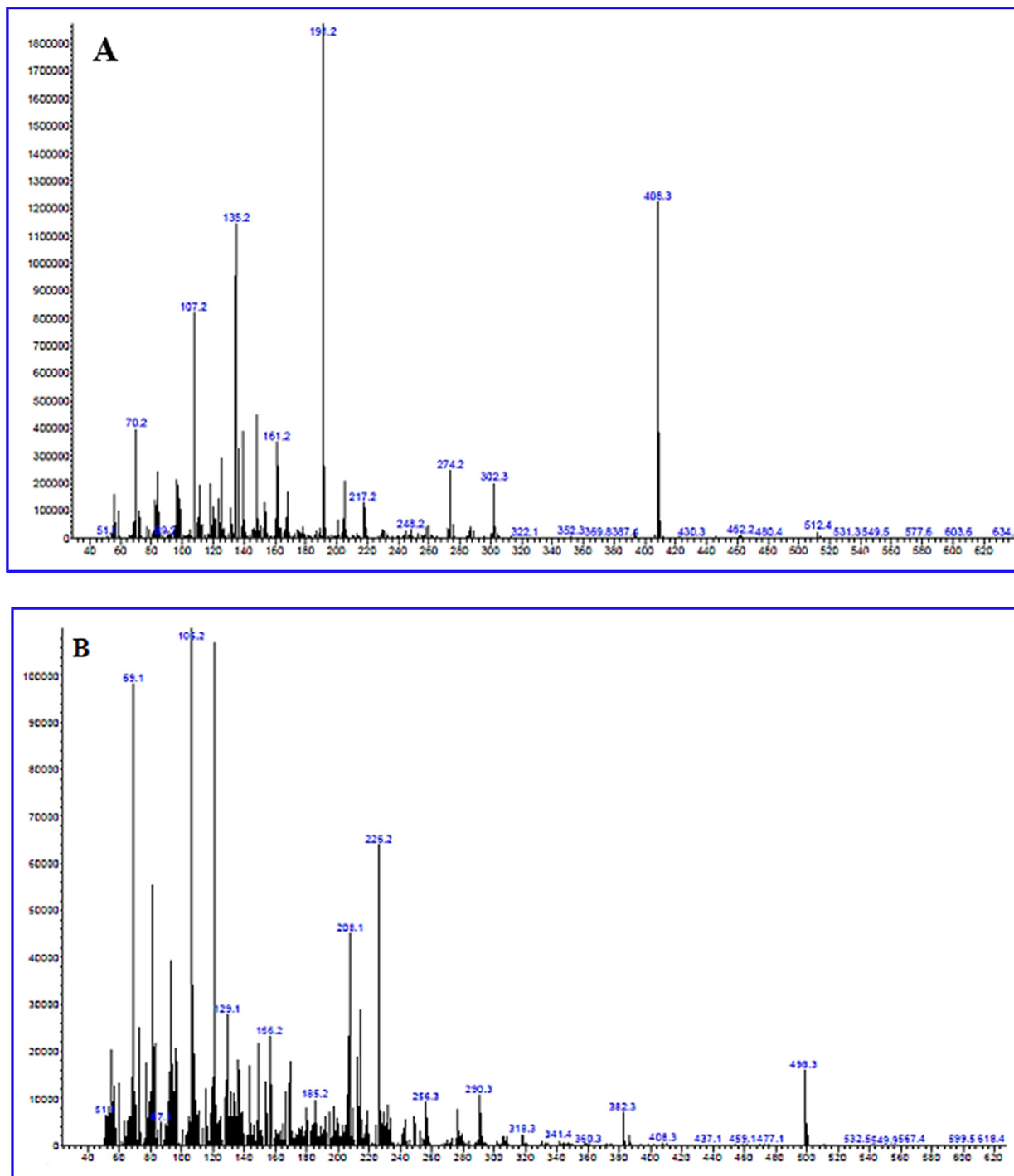


Fig. 1. Mass spectrum of ligand (A) and Pt(II) complex(B).

The mode of binding of the compounds with the double-stranded DNA would depend on a number of specific structural factors, including the charge on the compound, the size, the hydrogen-bonding capability and steric effects. The results here can be interpreted as an interaction between ct-DNA with the platinum complex and its ligand with a change in the conformation of the ct-DNA. The Wolfe-Shimmer equation (Eq. (1)) [52] was applied to calculate the intrinsic binding constant (K_b):

$$[DNA]/(\epsilon_a - \epsilon_f) = [DNA]/(\epsilon_b - \epsilon_f) + 1/K_b(\epsilon_a - \epsilon_f) \quad (1)$$

where [DNA] is the DNA concentration. ϵ_a is the apparent extinction coefficient, ϵ_f and ϵ_b represent the coefficient of extinction of the free complex and its completely DNA-bound compound, respectively. The intrinsic binding constant (K_b) was calculated by the slope to intercept ratio in the plot of $[DNA]/(\epsilon_a - \epsilon_f)$ against [DNA]. The K_b values of compounds (ligand: $4 \times 10^3 \text{ M}^{-1}$; platinum complex: $6.1 \times 10^4 \text{ M}^{-1}$) were calculated. The K_b value of the ligand indicated that the ligand could be interacting with ct-DNA via a groove binding mode [53]. The value of K_b ($6.1 \times 10^4 \text{ M}^{-1}$) of the complex could be compared with the values obtained for other

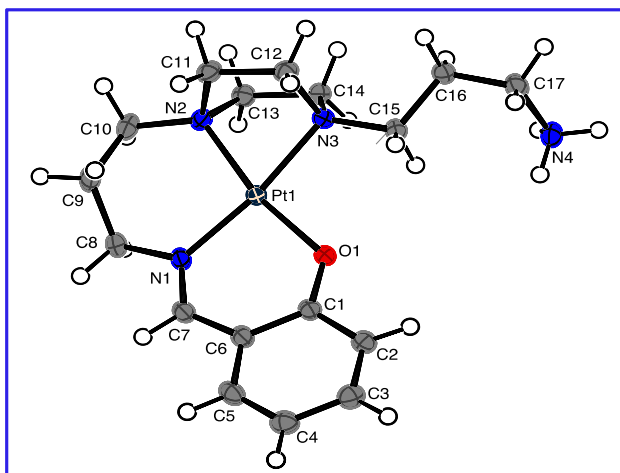


Fig 2. ORTEP diagram of the $[C_{17}H_{28}N_4OPt]^{2+}$ cation. Ellipsoids are drawn at the 70% probability level.

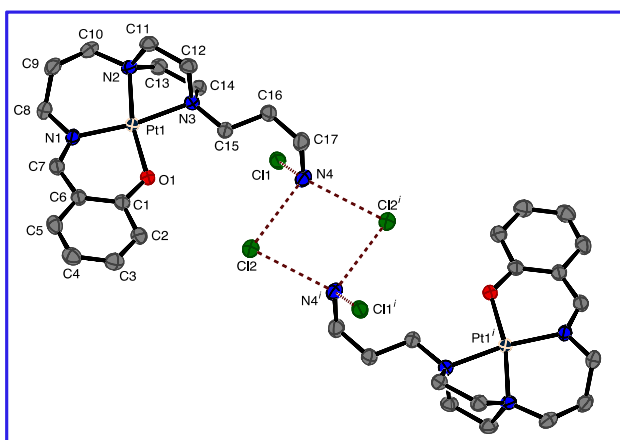


Fig 3. ORTEP diagram of the $[C_{17}H_{28}N_4OPt]Cl_2$ showing the hydrogen bonding between the chloride anions and the terminal amines. Ellipsoids are drawn at the 70% probability level. Hydrogen atoms are omitted for clarity.

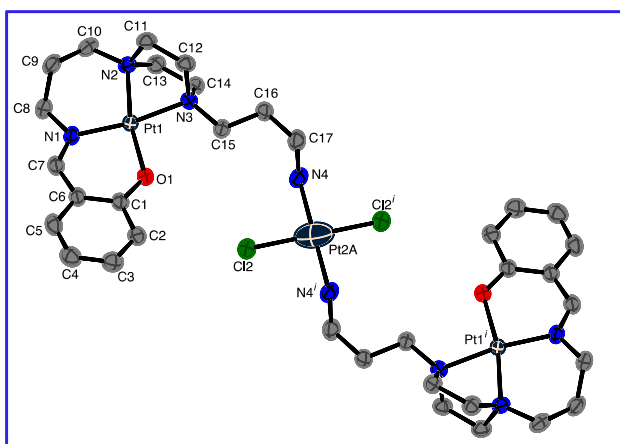


Fig 4. ORTEP diagram of the $[C_{17}H_{27}N_4OPt]_2Pt^{2+}$ cation. Ellipsoids are drawn at the 70% probability level. Hydrogen atoms are omitted for clarity.

intercalators like methylene blue ($2.13 \times 10^4 M^{-1}$); EtBr ($6.58 \times 10^4 M^{-1}$); acridine orange ($2.69 \times 10^4 M^{-1}$) and $[Pt(terpy)(OH)]^+(7 \times 10^4 M^{-1})$ [54,55]. Also, the constant value of

Table 2

Bond lengths (Å) and angles (°) for $0.973[C_{17}H_{28}N_4OPt]Cl_2 \cdot 0.014[[C_{17}H_{27}N_4OPt]_2PtCl_2]Cl_2$.

Bond	Length(Å)	Bond	Angle/
Pt1-O1	1.9964(18)	O1-Pt1-N2	168.02(8)
Pt1-N1	1.983(2)	O1-Pt1-N3	95.13(8)
Pt1-N2	2.045(2)	N1-Pt1-O1	92.66(8)
Pt1-N3	2.076(2)	N1-Pt1-N2	99.10(9)
O1-C1	1.315(3)	N1-Pt1-N3	171.53(9)
N1-C7	1.294(3)	N2-Pt1-N3	73.00(8)
Pt2A-N4	2.087(2)	C1-O1-Pt1	125.28(16)
Pt2A-Cl2	2.2898(7)	C7-N1-Pt1	124.30(18)
		C7-N1-C8	117.4(2)
		C8-N1-Pt1	118.28(16)
		N4 ⁱ -Pt2A-N4	180
		N4 ⁱ -Pt2A-Cl2	90.24(7)
		N4-Pt2A-Cl2	89.76(7)
		Cl2 ⁱ -Pt2A-Cl2	180

Symmetry Code: ⁱ 1-x, -y, 1-z

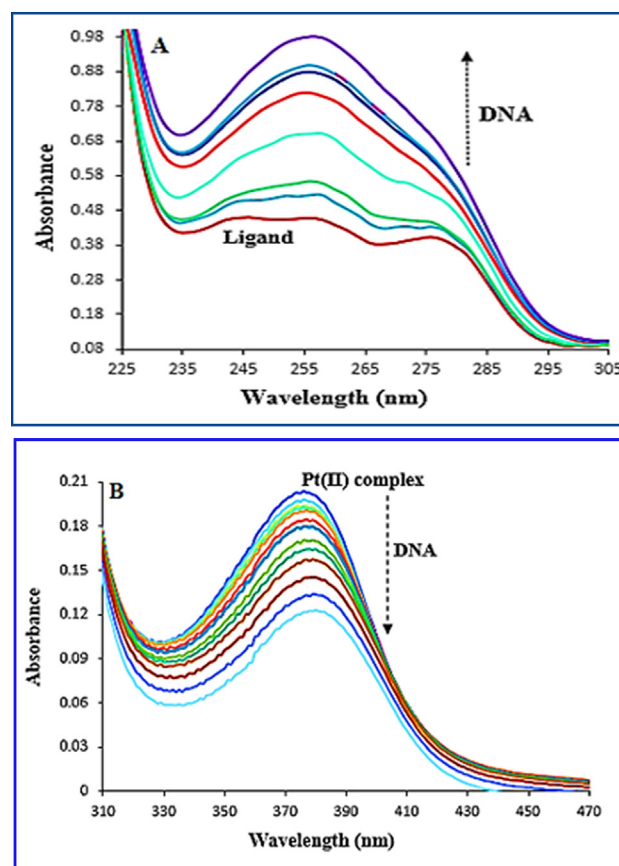


Fig 5. Absorption spectra of ligand (H_2L) ($2.43 \times 10^{-5} M$) (A) and $[C_{17}H_{28}N_4OPt]Cl_2$ complex ($1.5 \times 10^{-4} M$) (B) in the absence and presence of increasing amounts of ct-DNA.

intrinsic binding is similar to DNA groove binders like Tartrazine ($3.75 \times 10^4 M^{-1}$) [56]; isatin ($7.32 \times 10^4 M^{-1}$) [57]; and $[Pt(Met)(DMSO)Cl]Cl$ ($1.5 \times 10^4 M^{-1}$) [58]. The obtained values of K_b revealed that the binding of the platinum complex to ct-DNA is significantly stronger than that of the free ligand [59] and that the Pt (II) complex is bonding to ct-DNA via a partial intercalation mode, which includes both intercalation and groove binding modes.

3.2.2. Competitive fluorescence studies

The titration experiments of fluorescence were also carried out to study the mode of interaction of ct-DNA with both the ligand (H_2L) and the Pt(II) complex. Since there is no luminescence from

either the ligand or the Pt(II) complex, monitoring their interaction with DNA can be very difficult using direct fluorescence emission methods. However, it is possible to do so by indirect means, i.e., using a fluorescent organic molecule as a probe. To monitor the ligand and Pt(II) complex interaction with DNA methylene blue and Hoechst 33,258 were used as intercalator probe [60,61] and groove binder [62], respectively. As a sensitive fluorescence probe, Hoechst can fit into the groove sites of DNA [63]. Fig. 6A and B indicate the fluorescence spectra of a 5×10^{-6} M solution of the probe in the presence of constant concentrations of ct-DNA (ligand: 2.3×10^{-2} M; complex: 1.5×10^{-4} M) in the presence and absence of the ligand and the Pt(II) complex. The fluorescence emission intensity of Hoechst increased with increasing amounts of DNA. When this was done in the presence of ligand, or Pt complex, the results showed that increasing the concentration of the ligand (0 to 4.63×10^{-5} M) or the Pt complex (0 to 1.45×10^{-4} M) in the DNA-Hoechst solution, resulted in a decrease in the DNA-Hoechst fluorescence intensity. The fluorescence spectra indicate that the compounds do not react with the Hoechst molecules. It does, however, indicate that the addition of the complex or the ligand to a DNA-Hoechst solution results in them coordinating to the DNA molecules, with the Hoechst molecules being released into solution leading to a decrease of the fluorescence arising from the Hoechst-DNA complex. The observation of an isosbestic point at 451 nm and 466 nm in the ligand and complex spectra, respectively, can be regarded as a sign of the generation at least two species in equilibrium in solution (free and DNA-bound species) [64].

In order to get more information about the binding mode, additional competitive experiments were performed by applying probes like methylene blue. Methylene blue, as a sensitive fluorescence probe, can bind to the intercalation sites of the DNA helix. As

evident in the experiments, the intensity of the emission was reduced by increasing the DNA concentration. The experiments were performed via the titration of a 4.97×10^{-6} M solution of the probe, in various concentrations of ct-DNA, in the absence and presence of the Pt(II) complex or the ligand. Fig. 7A shows that the intensity of fluorescence of the probe falls on increasing the concentration of DNA. As the Pt(II) complex was added to the solution at concentrations of up to 8.16×10^{-5} M, there is a change in the MB-DNA interaction, with the methylene blue molecules binding to the DNA helix being replaced by molecules of the Pt(II) complex showing that the Pt(II) complex is also binding to the DNA in an intercalative mode. Fig. 7B shows the fluorescence emission spectra that result from the addition of the ligand to the MB-DNA system. There is no remarkable substitution of MB by ligand, which supports the view that the ligand is binding to the DNA via a non-interactive mode. The results of both experiments suggest that the adding of the Pt(II) complex to the DNA-Hoechst and DNA-MB complexes in solution results in the Pt(II) complex binding to the DNA replacing the Hoechst and MB molecules which are then released into the solution. As all of the methylene blue (a classical intercalator) and all of the Hoechst (a groove binder) molecules are released into solution, after the addition of the Pt(II) complex, it suggests that the Pt(II) complex can act as both an intercalator and a groove binder modes with DNA molecules (partial intercalation mode).

3.2.3. Determination of quenching mechanism

Quenching can occur via several mechanisms, namely, static and dynamic quenching. Contact between the quenching species and the excited fluorophore indicates dynamic quenching, while forming a complex with the stable ground state, which results an interaction between the complex and the labeled DNA is static

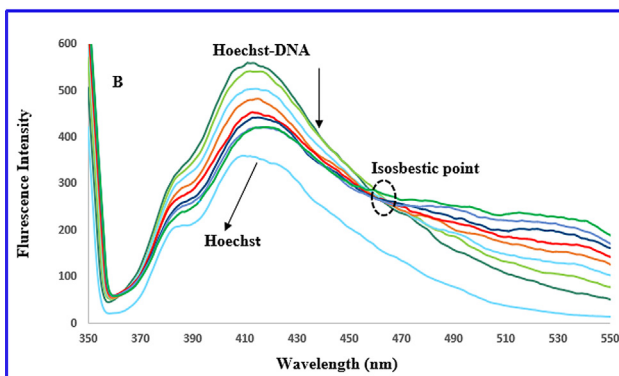
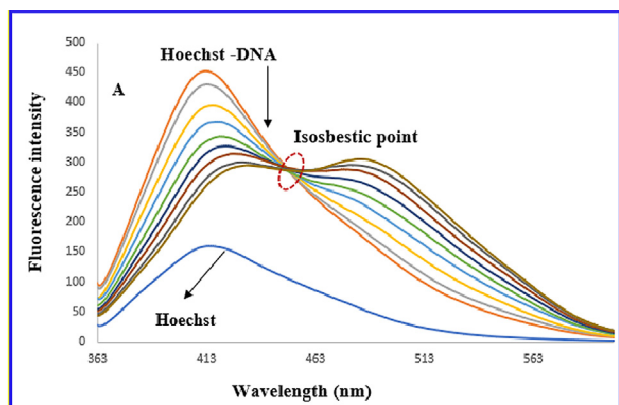


Fig. 6. Fluorescence spectra of the competition between Hoechst 33,258 (5×10^{-6} M) bound to DNA (2.3×10^{-2} M) with increasing the concentration of ligand to 4.63×10^{-5} M (A) and Pt(II) complex (B) $C_{DNA} = 1.5 \times 10^{-4}$ M, $C_{Pt(II) \text{ complex}} = (0-1.45 \times 10^{-4}$ M) at 288 K.

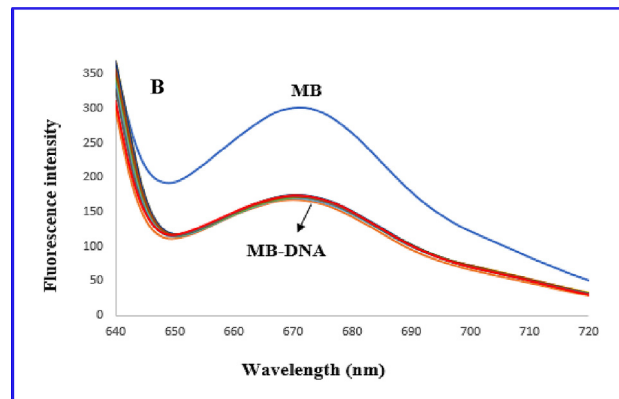
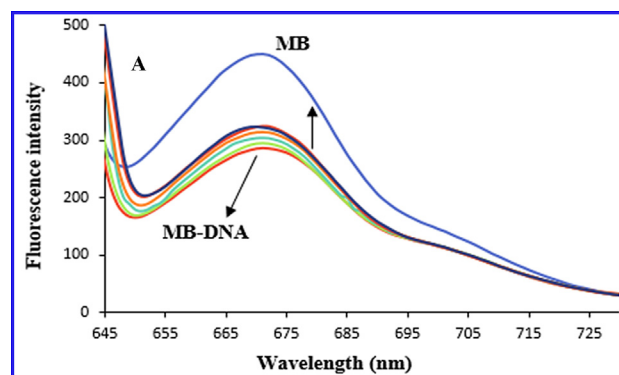


Fig. 7. Fluorescence spectra of the competition between MB (4.97×10^{-6} M) bound to DNA (6.48×10^{-5} M) with increasing the concentration of Pt(II) complex to 8.16×10^{-5} M (A) and ligand (B) $C_{DNA} = 3.38 \times 10^{-3}$ M, $C_{ligand} = (0-6.94 \times 10^{-5}$ M) at 298 K.

quenching. These two mechanisms depend on the temperature of the reaction medium and can be discerned by investigating the quenching that occurs at various temperatures. It is also of note that higher temperatures will lead to enhance diffusion and higher values of the dynamic quenching constant, while the static quenching constant will decrease at high temperatures [65]. The Stern–Volmer linear equation describes the fluorescence quenching (Eq. (2)):

$$F_0/F = 1 + K_q \tau_0 [Q] = 1 + K_{sv} [Q] \quad (2)$$

where F_0 and F are the fluorescence intensities in the absence and presence of quencher, respectively. $[Q]$ and K_{sv} refer to the complex concentration of quencher and quenching constant, K_q and τ_0 are the fluorophore constant and the lifetime in the absence of the quencher ($\tau_0=10^{-8}$), respectively [66]. According to the results in Table 3, the quenching mechanism for both the ligand and Pt(II) complex is static quenching as, when the temperature is increased, there is a decrease in K_{sv} [67].

Using the fluorescence titration data, the binding constant (K_f) and the number of the binding sites (n) that result from the complex of ct-DNA with compounds can be determined by the following (Eq. (3)) [68].

$$\log(F_0 - F)/F = \log K_f + n \log [Q] \quad (3)$$

The fluorescence intensities of the fluorophore can be regarded as F_0 and F in the absence and the presence of various quencher $[Q]$ concentrations. For the present compounds, when the temperature increased from 288 K to 310 K, the binding constant (K_f) of both the ligand and the Pt(II) complex decreased (Table 4). The obtained values of K_f , K_{sv} , and K_q of the Pt(II) complex indicated that it has a higher DNA binding activity than the free ligand.

3.2.4. Thermodynamic studies

There are a number of specific interactions between a biomolecule and the target compounds, including hydrogen bonds, electrostatic interactions, van der Waals interactions and hydrophobic forces. The results of thermodynamic studies (enthalpy changes (ΔH°) and entropy changes (ΔS°)) can help to determine the model of the interactions that have occurred between the target compound with a biomolecule [69]. There are three main models: (1) if $\Delta S^\circ < 0$ and $\Delta H^\circ < 0$, then hydrogen bonds and van der Waals interactions dominate; (2) if $\Delta S^\circ > 0$ and $\Delta H^\circ < 0$, then electrostatic interactions dominate; (3) if $\Delta S^\circ > 0$ and $\Delta H^\circ > 0$, then hydrophobic forces dominate [70]. The Van't-Hoff–Hoff equation (Eq. (4)), expressing how the equilibrium constant is dependent on temperature, can be used in determining the thermodynamic parameters of equilibrium [71]:

$$\Delta G^\circ = \Delta H^\circ - T \Delta S^\circ = -RT \ln K_f \quad (4)$$

where T and K_f are the temperature (K) and the constant of binding at the corresponding temperature and R is the universal gas constant ($R = 8.31 \text{ J.mol}^{-1}\text{K}$). As can be seen in Table 5, hydrogen bonds and van der Waals interactions are the most significant interactions when the ligand and the Pt(II) complex are binding to ct-DNA, as $\Delta S^\circ < 0$ and $\Delta H^\circ < 0$.

Table 3
The quenching constants of ligand (H₂L) and Pt(II) complex by ct-DNA at different temperatures.

ligand (H ₂ L)		Pt(II) complex				
T (K)	$K_{sv}(\text{L.mol}^{-1}) \times 10^3$	$K_q (\text{L.mol}^{-1}) \times 10^{11}$	R ²	$K_{sv}(\text{L}) \times \text{mol}^{-1} \cdot 10$	$K_q (\text{L.mol}^{-1}) \times 10^{11}$	R
288	1.154	1.154	0.997	2.223	2.223 ²	0.997
298	1.144	1.144	0.994	2.092	2.092	0.996
310	1.120	1.120	0.987	1.637	1.637	0.988

3.2.5. Viscosity measurements

Viscosity measurements are an easy assay to determine the mode of binding of compounds to ct-DNA, which can provide more information of the reactions between the ligand and the Pt(II) complex with DNA. The values of $(\eta/\eta_0)^{1/3}$ are plotted versus $1/R = [DNA]/[\text{compounds}]$, where η_0 and η are the DNA viscosity contributions in the absence (η_0) and in the presence of the compounds (η) (Fig. 8). For classical intercalation binding to occur there needs to be a large space close to the base pairs to incorporate the molecules and this causes increases the viscosity of the DNA [72]. In contrast, some molecules that can bind exclusively in the DNA grooves results to no or negligible change in the viscosity of the DNA solution [73]. Furthermore, under the same conditions mentioned above, exclusive binding of molecules through nonclassical and/or partial intercalation in the grooves of DNA can lead to no variation, or a small (negative or positive) variation, in the viscosity of the DNA solution [74]. The viscosity results here indicate that there are at least two binding phases that could be occurring between the ct-DNA and the Pt(II) complex. The viscosity declined at small complex concentrations, and then increased at high complex concentrations. This phenomenon is probably due to changes in the flexibility of the DNA molecule or to changes in the conformation. A slow increase in viscosity was observed with increasing concentration of ligand, showing that the ligand binds to DNA by the groove binding mode [75,76].

3.3. Molecular docking study

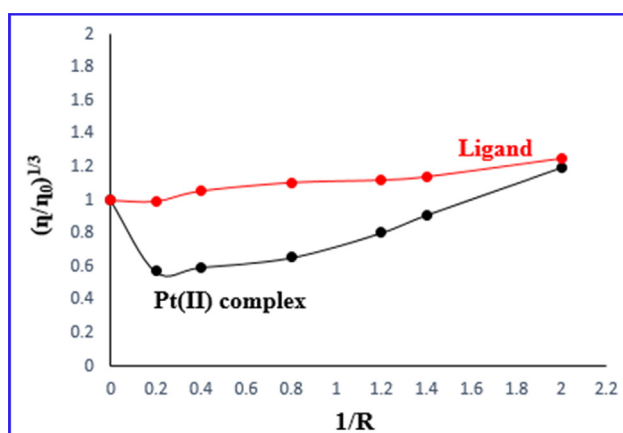
Computer docking calculations have been regarded as significant techniques in the elucidation of reactions mechanisms and in drug design. The flexible docking programs aim at predicting the structures of protein–ligand complexes quickly and accurately. Used before the experimental screening of the activities of target compounds, the docking programs are regarded as powerful filters aimed at reducing the time and cost of investigating and developing compounds of medicinal interest. When they are used after the experimental screening, they provide a better understanding of bioactivity mechanisms [77]. From the docking calculations, the best docking energy is taken from the 20 minimum energy conformers, obtained from 100 runs, as is shown in Fig. 9. As can be seen, the H₂L ligand binding site is situated in the DNA minor groove. From the docking maps, it is apparent that in the interaction of the ligand with DG2, DG24, DA5, and DC21 nucleobases, there are five hydrogen bonds formed at distances of between 2.20 and 2.70 Å (Fig. 9). According to the docking results, the platinum complex can be located in the double-helix DNA intercalation and groove sites (Fig. 10). The platinum complex has the ability to interact with the DNA by both the intercalation and groove modes, and had van der Waals interactions with the duplex DNA double strands. Fig. 10 shows that two hydrogen bonds were formed between the platinum complex and duplex DNA. The first one forms between the O2-DC-9 fragment of the DNA, and a hydrogen atom in the platinum complex, at a distance of 2.48 Å, while the second one is formed between the OP1-DG-10 fragment of the DNA a hydrogen atom in the platinum complex, at a distance of 2.11 Å. This indicates that the hydrogen bond with the O2 binding site of the DNA is less stable than the hydrogen bond involving the

Table 4
Binding constants (K_f) and number of binding sites (n) for interaction of ligand (H_2L) and Pt(II) complex with ct-DNA.

ligand (H_2L)				Pt(II) complex		
T (K)	n	K_f	R^2	n	K_f	R^2
288	0.93	5.37×10^3	0.999	1.14	1.51×10^4	0.998
298	0.91	3.37×10^3	0.988	0.96	2.27×10^3	0.997
310	0.89	3.16×10^3	0.992	0.90	1.58×10^3	0.987

Table 5
Thermodynamic parameters for the binding of ligand (H_2L) and Pt(II) complex to ct-DNA.

ligand (H_2L)				Pt(II) complex		
T (K)	ΔG° (kJ.mol $^{-1}$)	ΔH° (kJ.mol $^{-1}$)	ΔS° (J.mol $^{-1}$ k $^{-1}$)	ΔG° (kJ.mol $^{-1}$)	ΔH° (kJ.mol $^{-1}$)	ΔS° (J.mol $^{-1}$ k $^{-1}$)
288	-20.56	-17.80	-9.42	-22.49	-66.73	-154.37
298	-20.53			-20.53		
310	-20.77			-18.97		

**Fig. 8.** Effect of increasing amounts of the ligand and Pt(II) complex on the viscosity of ct-DNA (5×10^{-5} M) in 50 mM Tris-HCl buffer ($r_i = 0.0, 0.4, 0.6, 0.8, 1.0, 1.4, 2$).

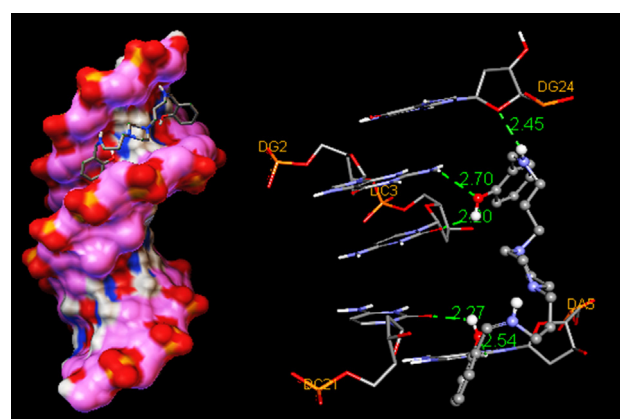
OP1 binding site. The (ΔG) for the platinum complex-DNA (-20.76 J. mol $^{-1}$) calculated from the docking simulation was found to be slightly lower than that found from the fluorescence data, which may be due to excluding the effects of receptor DNA rigidity and or the effects of the solvent.

3.4. Cytotoxicity activities

To examine the antiproliferative effect of the newly synthesized complex on prostate, skin, and cervix cancer cells, the MTT method was used to assess the complex daily exposure for the viability of these cells to determine the values of IC₅₀, in the range of $\mu\text{g/mL}$ (Fig. 11). The findings revealed that the complex of Pt(II) had a highly toxic effect against PC3 (IC₅₀ = 18.59 $\mu\text{g/mL}$) and moderate cytotoxic effects against A431 (IC₅₀ = 34.52 $\mu\text{g/mL}$) cell line in a dose-dependent manner. Moreover, based on the findings, the Pt (II) complex possessed a weak cytotoxic effect against Hela cancer cells. Generally, our results indicated that the synthesized compound had a remarkable cytotoxic effect on human prostate carcinoma cells.

4. Conclusion

In this paper, we described synthesis of a Schiff base ligand derived from a polyamine containing piperazine moiety and salicylaldehyde and the synthesis of the Pt(II) complex. This complex and its ligand were characterized by a number of analytical, spectroscopic and physicochemical methods. A single crystal X-ray

**Fig. 9.** Molecular docked models of energy-minimized structure of H_2L ligand with DNA (Left) and hydrogen-bonding interactions between ligand (ball and sticks) and DNA nucleobase (lines) (Right).

structural analysis was performed to a certain the molecular structure of the Pt(II) complex. During the crystallization process, the presence of a slight excess of Pt resulted in the crystal being composed of two different complexes which co-crystallized, the formulation being $0.973[C_{17}H_{28}N_4OPT]Cl_2$; $0.014[[C_{17}H_{27}N_4OPT]_2Pt Cl_2] Cl_2$, (1) and (2), respectively. In both structures, the metal atoms were in a square planar coordination environment. The binding of ct-DNA to the ligand and to the Pt(II) complex were also studied. Measurement of the UV-Vis spectra resulted in the determination of the binding constant of ligand (4×10^3 M $^{-1}$) and platinum complex (6.1×10^4 M $^{-1}$), which indicated the binding of the complex to DNA is stronger than for the free ligand. Competitive binding experiments, using methylene blue and Hoechst 33258, indicated that the ligand binds to the DNA via groove binding mode, while the Pt(II) complex reacts with molecules of ct-DNA via the mode of partial intercalation. Thermodynamic studies indicated that van der Waals interactions and hydrogen bonds could be regarded as the most significant interactions in the binding of the ligand and the Pt(II) complex to molecules of ct-DNA. The results of docking calculations, determining the optimal energy, confirmed that the Pt(II) complex could be placed in both groove and intercalation sites of the double-helix of DNA, while the ligand (H_2L) can only be found in the minor groove of DNA. Finally, the cytotoxicity studies showed that the Pt(II) complex showed outstanding cytotoxic effects on the carcinoma cells of the human prostate. The present study has enabled us to get important information on the mechanism of interaction between DNA and a new platinum complex,

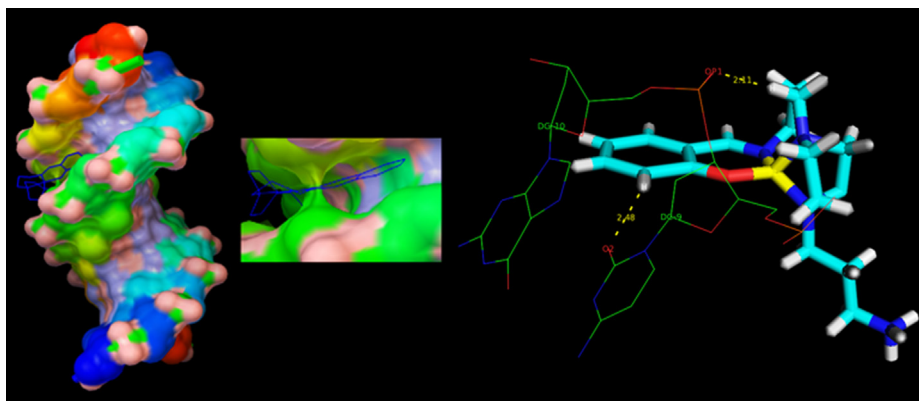


Fig. 10. Molecular docked models of energy-minimized structure of Pt(II) complex with DNA (Left) and hydrogen-bonding interactions between ligand (sticks) and DNA nucleobase (lines) (Right).

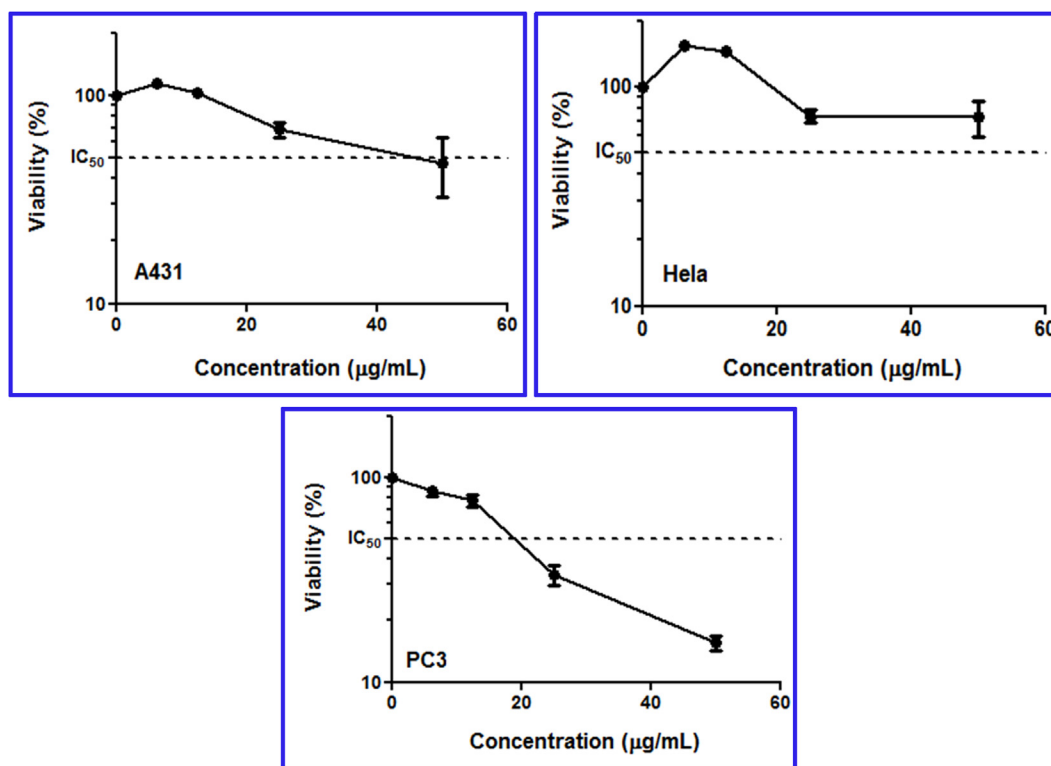


Fig. 11. Cell viability of A431, HeLa, and PC3 cell lines after 24 h treatment with different concentrations of Pt(II) complex. Data are expressed as Mean \pm S.E.M three experiments.

and also assists us in designing more efficient anticancer metallodrugs.

Declaration of Competing Interest

The authors declare that they have no known competing financial interests or personal relationships that could have appeared to influence the work reported in this paper.

Acknowledgements

With special thanks to the Faculty of Chemistry of Bu-Ali Sina University.

Appendix A. Supplementary data

Supplementary data to this article can be found online at <https://doi.org/10.1016/j.molliq.2021.116292>.

References

- [1] P.E.N. Barry, J.P. Sadler, Exploration of the medical periodic table: towards new targets, *Chem. Commun.* 49 (2013) 5106–5131, <https://doi.org/10.1039/C3CC41143E>.
- [2] Z.D. Bugar_cic, J. Bogojeski, B. Petrovi_c, S. Hochreuther, R. van Eldik, Mechanistic studies on the reactions of platinum (II) complexes with nitrogen and sulfur-donor biomolecules, *Dalton Trans.* 41 (2012) 12329e12345. <https://doi.org/10.1039/C2DT31045G>.
- [3] J.A. Cowan, Chemical nucleases, *Curr. Opin. Chem. Biol.* 5 (2001) 634–642, [https://doi.org/10.1016/S1367-5931\(01\)00259-9](https://doi.org/10.1016/S1367-5931(01)00259-9).
- [4] S. Mathur, S. Tabassum, Cent. New homodi- and heterotruclear metal complexes of Schiff base compartmental ligand: interaction studies of

- copper complexes with calf thymus DNA. *Eur. J. Chem.* 4 (2006) 502–522. <https://doi.org/10.2478/s11532-006-0020-6>.
- [5] P.M. Takahara, C.A. Frederick, S.J. Lippard, Crystal structure of the anticancer drug cisplatin bound to duplex DNA. *J Am Chem Soc* 118 (1996) 12309–12321, <https://doi.org/10.1021/ja9625079>.
- [6] P.J. Loehrer, L.H. Einhorn, Drugs five years later. Cisplatin. *Ann. Intern. Med.* 100 (1984) 704–713, <https://doi.org/10.7326/0003-4819-100-5-704>.
- [7] A. Garoufis, S.K. Hadjikakou, N. Hadjiliadis, Palladium coordination compounds as anti-viral, anti-fungal, anti-microbial and anti-tumor agents. *Coord. Chem. Rev.* 253 (2009) 1384, <https://doi.org/10.1016/j.ccr.2008.09.011>.
- [8] S. Medici, M. Peana, V.M. Nurchi, J.I. Lachowicz, G. Crisponi, M.A. Zoroddu, Metals in Medicine: Latest Advances *Coord. Chem. Rev.* 284 (2015) 329–350, <https://doi.org/10.1016/j.ccr.2014.08.002>.
- [9] W. Wang, Z. Guo, Targeting and delivery of platinum-based anticancer drugs. *Chem. Soc. Rev.* 42 (2013) 202, <https://doi.org/10.1039/C2CS35259A>.
- [10] M. Rezaeivala, H. Keypour, Schiff base and non-Schiff base macrocyclic ligands and complexes incorporating the pyridine moiety – The first 50 years. *Coord. Chem. Rev.* 280 (2014) 203–253, <https://doi.org/10.1016/j.ccr.2014.06.007>.
- [11] B.K. Panda, A. Chakravorty, Carbonylation of four-membered ruthenium and osmium metallacycles incorporating an orthometallated phenolic function: New acylruthenium and arylsodium complexes. *J. Organomet. Chem.* 690 (2005) 3169–3175, <https://doi.org/10.1016/j.jorganchem.2005.04.012>.
- [12] K.R. Krishnapriya, M. Kandaswamy, Coordination properties of a dicompartmental ligand with tetra- and hexadentate coordination sites towards copper (II) and nickel (II) ions. *Polyhedron* 24 (2005) 113–120, <https://doi.org/10.1016/j.poly.2004.10.010>.
- [13] K.N. Kumar, R. Ramesh, Synthesis of lanthanide(III) complexes of chloro- and bromo substituted 18-membered tetraaza macrocycles. *Polyhedron* 18 (1999) 1561–1568, [https://doi.org/10.1016/S0277-5387\(99\)00016-9](https://doi.org/10.1016/S0277-5387(99)00016-9).
- [14] H. Keypour, N. Ansari, M. Mahmoudabadi, R. Karamian, S.H.M. Farida, M.E. Moghadam, R.W. Gable, Mn(III), Zn(II) and Pt(II) macrocyclic complexes: Synthesis, X-ray structures, anticancer and antioxidant activities. *Inorganica Chim. Acta.* 509 (2020), <https://doi.org/10.1016/j.ica.2020.119705> 119705.
- [15] P. Das, W. Linert, Schiff base-derived homogeneous and heterogeneous palladium catalysts for the Suzuki-Miyaura reaction. *Coord. Chem. Rev.* 311 (2016) 1–23, <https://doi.org/10.1016/j.ccr.2015.11.010>.
- [16] P. Rathelot, P. Vanelle, M. Gasquet, F. Delmas, M.P. Crozet, P. Timon-David, J. Maldonado, Synthesis of novel functionalized 5-nitroisquinolines and evaluation of in vitro antimalarial activity. *Eur. J. Med. Chem.* 30 (1995) 503–508, [https://doi.org/10.1016/0223-5234\(96\)88261-4](https://doi.org/10.1016/0223-5234(96)88261-4).
- [17] H. Keypour, M.T. Rezaei, M. Jamshidi, S. H. M. Farida, R. Karamian, Synthesis, cytotoxicity, and antioxidant activity by in vitro and molecular docking studies of asymmetrical diamine containing piperazine moiety and related Zn(II), Cd(II) and Mn(II) macrocyclic schiff base complexes. *J. Inorg. Chem. Commun.* 125 (2021) 108443. <https://doi.org/10.1016/j.inoche.2021.108443>.
- [18] Y.H. Ebead, H.M. Salman, M.A. Abdellah, Experimental and theoretical investigations of spectral, tautomerism and acid-base properties of Schiff bases derived from some amino acids. *Bull. Korean Chem. Soc.* 31 (2010) 850–858, <https://doi.org/10.5012/bkcs.2010.31.04.850>.
- [19] B. Ifrikhar, J. Kanwal, M. S. U. Khan, Z. Akhter, B. Mirza, V. Mckee, Synthesis, characterization and biological assay of Salicylaldehyde Schiff base Cu(II) complexes and their precursors. *J. Mol. Struct.* 1155 (2018) 337–348. <https://doi.org/10.1016/j.molstruc.2017.11.022>.
- [20] M.M. Omar, G.G. Mohamed, A.A. Ibrahim, Spectroscopic characterization of metal complexes of novel Schiff base. Synthesis, thermal and biological activity studies. *Spectrochim. Acta A Mol. Biomol. Spectrosc.* 73 (2009) 358–369, <https://doi.org/10.1016/j.saa.2009.02.043>.
- [21] F.-U. Rahman, A. Ali, I.U. Khan, H.-Q. Duong, S.-B. Yu, Y.-J. Lin, H. Wang, Z.-T. Li, D.-W. Zhang, Morpholine or methylpiperazine and salicylaldehyde based heteroleptic square planar platinum (II) complexes: In vitro anticancer study and growth retardation effect on *E. coli*. *Eur. J. Med. Chem.* 131 (2017) 263–374, <https://doi.org/10.1016/j.ejmech.2017.03.014>.
- [22] H. Keypour, M. Shayesteh, A. Sharifi-Rad, S. Salehzadeh, H. Khavasi, L. Valencia, Synthesis and characterization of copper(II) and cobalt(II) complexes with two new potentially hexadentate Schiff base ligands. X-ray crystal structure determination of one copper(II) complex. *J. Organomet. Chem.* 693 (2008) 3179, <https://doi.org/10.1016/j.jorganchem.2008.07.012>.
- [23] H. Keypour, R. Azadbakht, S. Salehzadeh, H. Khanmohammadi, H. Khavasi, H. Adams, Synthesis, crystal structure and spectroscopic properties of some cadmium(II) complexes with three polyamine and corresponding macrocyclic Schiff base ligands. *J. Organomet. Chem.* 693 (2008) 2237, <https://doi.org/10.1016/j.jorganchem.2008.03.025>.
- [24] H. Keypour, M. Rezaeivala, L. Valencia, P. Pérez-Lourido, H.R. Khavasi, Synthesis and characterization of some new Co(II) and Cd(II) macrocyclic Schiff-base complexes containing piperazine moiety. *Polyhedron* 28 (2009) 3755, <https://doi.org/10.1016/j.poly.2009.08.021>.
- [25] H. Keypour, M. Rezaeivala, L. Valencia, S. Salehzadeh, P. Pérez-Lourido, H.R. Khavasi, Synthesis and crystal structure of some new cadmium (II) macrocyclic Schiff-base complexes containing piperazine moiety. *Polyhedron* 28 (2009) 3533–3541, <https://doi.org/10.1016/j.poly.2009.05.083>.
- [26] H. Keypour, M. Rezaeivala, L. Valencia, P. Pérez-Lourido, A.H. Mahmoudkhani, Synthesis and characterization of two zinc(II) macrocyclic Schiff-base complexes containing piperazine moiety, crystal structure of one complex. *Polyhedron* 28 (2009) 3415–3418, <https://doi.org/10.1016/j.poly.2009.07.012>.
- [27] H. Keypour, M. Rezaeivala, A. Ramezani-Aktij, M. Bayat, N. Dilek, H. Ünver, New macrocyclic schiff base complexes incorporating a homopiperazine unit: Synthesis of some Co(II), Ni(II), Cu(II) and Zn(II) complexes and crystal structure and theoretical studies. *J. Mol. Struct.* 1115 (2016) 180–186, <https://doi.org/10.1016/j.molstruc.2016.02.071>.
- [28] H. Keypour, M. Mahmoudabadi, A. Shooshtari, M. Bayat, R. Karamian, M. Asadbeg, R.W. Gable, Synthesis, crystal structure, theoretical studies and biological properties of three novel trigonal prismatic Co(II), Ni(II) and Cu(II) macrocyclic Schiff base complexes incorporating piperazine moiety. *Inorg. Chim. Acta.* 478 (2018) 176–186, <https://doi.org/10.1016/j.ica.2018.02.028>.
- [29] H. Keypour, M. Rahpeyma, M. Rezaeivala, P. Arzhangi, M. Bayat, L. Valencia, Y. Elerman, O. Büyükgüngör, Synthesis and structural characterization of a new Schiff base macrocyclic ligand containing a piperazine head unit and its metal complexes. Crystal structure of the Co(II) complex. *Polyhedron.* 51 (2013) 117–122, <https://doi.org/10.1016/j.poly.2012.12.020>.
- [30] H. Keypour, M. Rezaeivala, M. Mirzaei-Monsef, K. Sayin, N. Dilek, H. Ünver, Synthesis and characterization of Co(II), Ni(II), Cu(II) and Zn(II) complexes with a new homopiperazine macrocyclic Schiff base ligand. *Inorg. Chim. Acta.* 440 (2015) 139, <https://doi.org/10.1016/j.ica.2015.04.017>.
- [31] H.M. Niemeyer, Conformational equilibria in six-membered rings. *J. Mol. Struct.* 57 (1979) 241, [https://doi.org/10.1016/0022-2860\(79\)80249-5](https://doi.org/10.1016/0022-2860(79)80249-5).
- [32] H. Keypour, M. Rezaeivala, L. Valencia, P. Pérez-Lourido, Synthesis and crystal structure of Mn(II) complexes with novel macrocyclic Schiff-base ligands containing piperazine moiety. *J. Polyhedron* 27 (2008) 3172, <https://doi.org/10.1016/j.poly.2008.07.012>.
- [33] J. Marmur, A procedure for the isolation of deoxyribonucleic acid from microorganisms. *J. Mol. Biol.* 3 (1961) 585, [https://doi.org/10.1016/S0022-2836\(61\)80047-8](https://doi.org/10.1016/S0022-2836(61)80047-8).
- [34] M.E. Reichmann, S.A. Rice, C.A. Thomas, P. Doty, A Further Examination of the Molecular Weight and Size of Desoxyribose Nucleic Acid. *J. Am. Chem. Soc.* 76 (1954) 3047, <https://doi.org/10.1021/ja01640a067>.
- [35] N. Shahabadi, L. Heidari Synthesis, characterization and multi-spectroscopic DNA interaction studies of a new platinum complex containing the drug metformin. *Spectrochimica Acta Part A: Molecular and Biomolecular Spectroscopy* 128 (2014) 377–385. <https://doi.org/10.1016/j.saa.2014.02.167>.
- [36] G.M. Morris, R. Huey, W. Lindstrom, M.F. Sanner, R.K. Belew, D.S. Goodsell, A.J. Olson, AutoDock4 and AutoDockTools4: Automated docking with selective receptor flexibility. *J. Comput. Chem.* 30 (2009) 2785–2791, <https://doi.org/10.1002/jcc.21256>.
- [37] G.M. Morris, R. Huey, A.J. Olson, Using Auto Dock for ligand-receptor docking. *Curr. Protoc. Bioinf.* 8 (2008) unit 14.1–14.18. <https://doi.org/10.1002/0471250953.bi0814s24>.
- [38] W.L. DeLano, The PyMOL Molecular Graphics System, DeLano Scientific, San Carlos, CA, USA, 2004. <<http://pymol.sourceforge.net/>>.
- [39] Y. Luo, F. Xiao, S. Qian, W. Lu, B. Yang, Synthesis and in vitro cytotoxic evaluation of some thiazolylbenzimidazole derivatives. *Eur. J. Med. Chem.* 46 (1) (2011) 417–422, <https://doi.org/10.1016/j.ejmech.2010.11.014>.
- [40] H. Keypour, F. Forouzandeh, S. Salehzadeh, F. Hajibabaei, S. Feizi, R. Karamian, N. Ghiasi, R. W. Gable, DNA binding studies and antibacterial properties of a new Schiff base ligand containing homopiperazine and products of its reaction with Zn(II), Cu(II) and Co(II) metal ions: X-ray crystal structure of Cu(II) and Zn(II) complexes. *J. Polyhedron*, 170 (2019) 584–592. <https://doi.org/10.1016/j.poly.2019.06.023>.
- [41] J.H. Price, A.N. Williamson, R.F. Schramm, B.B. Wayland, Palladium(II) and Platinum(II) Alkyl Sulfoxide Complexes. Examples of Sulfur-Bonded, Mixed Sulfur and Oxygen-Bonded, and Totally Oxygen-Bonded Complexes. *J. Inorg. Chem.* 11 (6) (1972) 1280–1284, <https://doi.org/10.1021/ic50112a025>.
- [42] O.V. Dolomanov, L.J. Bourhis, R.J. Gildea, J.A.K. Howard, H. Puschmann, OLEX2: a complete structure solution, refinement and analysis program. *J. Appl. Cryst.* 42 (2009) 339–341, <https://doi.org/10.1107/S0021889808042726>.
- [43] G.M. Sheldrick, SHELXT— Integrated space-group and crystal-structure determination. *Acta Cryst. A* 71 (2015) 3–8, <https://doi.org/10.1107/S2053273314026370>.
- [44] G.M. Sheldrick, Crystal structure refinement with SHELXL. *Acta Cryst. C* 71 (2015) 3–8, <https://doi.org/10.1107/S2053229614024218>.
- [45] D. Tran Bui, V. Duong Ba, M. Khoi Nguyen Hoang, T. Vu Quoc, L. Duong Khanh, Y. Oanh Doan Thi, L. Van Meervelt, Synthesis and redetermination of the crystal structure of salicylaldehyde N (4)-morpholiniothiosemicarbazone. *Acta Cryst.* (2019) E75, 1389–1393. <https://doi.org/10.1107/S2056989019011812>.
- [46] N.S. Gill, R.H. Nutall, D.E. Scaife, The infra-red spectra of pyridine complexes and pyridinium salt. *J. Inorg. Nucl. Chem.* 18 (1961) 79, [https://doi.org/10.1016/0022-1902\(61\)80372-2](https://doi.org/10.1016/0022-1902(61)80372-2).
- [47] R. Melanson, F.D. Rochon, trans-Bis(tert-butylamine)dichloroplatinum(II), C8H22Cl2N2Pt, *Acta Cryst. Sect. C: Struct. Commun.* 41(1985) 350–352. <https://doi.org/10.1107/S0108270185003870>.
- [48] E.C. Long, J.K. Barton, On demonstrating DNA intercalation. *Acc. Chem. Res.* 23 (1990) 271–273, <https://doi.org/10.1021/ar00177a001>.
- [49] Y.J. Liu, X.Y. We, F.H. Wu, W.J. Mei, L.X. He, Interaction studies of DNA binding of ruthenium (II) mixedligand complexes: [Ru(phen)₂(dtni)]²⁺ and [Ru(phen)₂(dtni)]²⁺. *Spectrochim. Acta Part A* 70 (2008) 171–176, <https://doi.org/10.1016/j.saa.2007.07.029>.
- [50] R. Marty, N.Ch. Nsoukpoe-Kossi, D. Charbonneau, C.M. Weinert, L. Kreplak, H.A. Tajmir-Riahi, Structural analysis of DNA complexation with cationic lipids. *Nucleic Acids Res.* 37 (2009) 849–857, <https://doi.org/10.1093/nar/gkn1003>.
- [51] K.Y. Choi, Synthesis, properties and X-ray crystal structures of nickel(II) complexes of hexaazamacrotetracyclic ligand. *J. Coord. Chem.* 56 (2010) 481–491, <https://doi.org/10.1080/0095897031000100016>.

- [52] M. Sankarganesh, S.R. Vijay, J.D. Raja, Platinum complex with pyrimidine and morpholine based ligand: Synthesis, spectroscopic, DFT, TDDFT, catalytic reduction, *in vitro* anticancer, antioxidant, antimicrobial, DNA binding and molecular modeling studies, *J. Biomol. Struct. Dyn.* 39 (2020) 1055–1067, <https://doi.org/10.1080/07391102.2020.1727364>.
- [53] C. Kalaivanan, M. Sankarganesh, M.Y. Suvaikin, G.B. Karthi, S. Gurusamy, R. Subramanian, R.N. Asha, Novel Cu(II) and Ni(II) complexes of nicotinamide based Mannich base: Synthesis, characterization, DFT calculation, DNA binding, molecular docking, antioxidant, antimicrobial activities, *J. Mol. Liq.* 320 (2020), <https://doi.org/10.1016/j.molliq.2020.114423>.
- [54] S. Nafisi, A.A. Saboury, N. Keramat, J.F. Neault, H.A. Tajmir-Riahi, Stability and structural features of DNA intercalation with ethidium bromide, acridine orange and methylene blue, *J. Mol. Struct.* 827 (2008) 35–43, <https://doi.org/10.1016/j.molstruc.2006.05.004>.
- [55] S. Kashanian, S. Heidary Zeidali, DNA Binding Studies of Tartrazine Food Additive, *DNA Cell Biol.* 30 (2011) 499–505, <https://doi.org/10.1089/dna.2010.1181>.
- [56] S.D. Cummings, Platinum complexes of terpyridine: Interaction and reactivity with biomolecules, *J. Coord. Chem. Rev.* 253 (2009) 1495–1516, <https://doi.org/10.1016/j.ccr.2008.12.009>.
- [57] Nahid Shahabadi, Leila Heidari Synthesis, characterization and multi-spectroscopic DNA interaction studies of a new platinum complex containing the drug metformin, *J. Spectrochim. Acta Part A: Mol. Biomol. Spectrosc.* 128 (2014) 377–385, <https://doi.org/10.1016/j.saa.2014.02.167>.
- [58] S. Kashanian, M.M. Khodaie, P. Pakravan, Spectroscopic Studies on the Interaction of Isatin with Calf Thymus DNA, *DNA Cell Biol.* 29 (2010) 639–649, <https://doi.org/10.1089/dna.2010.1054>.
- [59] P.A. Jose, M. Sankarganesh, J.D. Raja, S.S. Saleem, Pyrimidine Derivative Schiff Base Ligand Stabilized Copper and Nickel Nanoparticles by Two Step Phase Transfer Method; *in Vitro* Anticancer, Antioxidant, Anti-Microbial and DNA Interactions, *J. Fluoresc.* 30 (2020) 471–482, <https://doi.org/10.1007/s10895-020-02510-5>.
- [60] P. Vardevanyan et al., Mechanisms for binding between methylene blue and DNA, *J. Appl. Spectrosc.* 80 (4) (2013) 595–599, <https://doi.org/10.1007/s10812-013-9811-7>.
- [61] E.T. Wahyuni et al., Spectroscopic studies on the thermodynamic and thermal denaturation of the ct-DNA binding of methylene blue, *Spectrochim. Acta A Mol. Biomol. Spectrosc.* 77 (2) (2010) 528–534, <https://doi.org/10.1016/j.saa.2010.06.032>.
- [62] M.C. Vega et al., Three-dimensional crystal structure of the A tract DNA dodecamer d (CGCAAATTTGCG) complexed with the minor groove binding drug Hoechst 33258, *Eur. J. Biochem.* 222 (1994) 721–726, <https://doi.org/10.1111/j.1432-1033.1994.tb18917.x>.
- [63] D. Stout, F. Becker, Fluorometric quantitation of single-stranded DNA: a method applicable to the technique of alkaline elution, *Anal. Biochem.* 127 (2) (1982) 302–307, [https://doi.org/10.1016/0003-2697\(82\)90177-4](https://doi.org/10.1016/0003-2697(82)90177-4).
- [64] N. Revathi, M. Sankarganesh, J.D. Raja, V.K.G. Gangatharan, S. Arumugam, R. Rajasekaran, Bioactive mixed ligand Cu(II) and Zn(II) complexes of pyrimidine derivative Schiff base: DFT calculation, antimicrobial, antioxidant, DNA binding, anticancer and molecular docking studies, *J. Biomol. Struct. Dyn.* 5 (2020) 1–13, <https://doi.org/10.1080/07391102.2020.1759454>.
- [65] Y. Sun, S. Bi, D. Song, C. Qiao, D. Mu, H. Zhang, Sens. Study on the interaction mechanism between DNA and the main active components in *Scutellaria baicalensis* Georgi, *J. Sens. Actuators B Chem.* 129 (2008) 799–810, <https://doi.org/10.1016/j.snb.2007.09.082>.
- [66] F.L. Cui, J. Fan, J.P. Li, Z.D. Hu, Bioorg. Interactions between 1-benzoyl-4-p-chlorophenyl thiosemicarbazide and serum albumin: investigation by fluorescence spectroscopy, *J. Med. Chem.* 12 (2004) 151–157, <https://doi.org/10.1016/j.bmc.2003.10.018>.
- [67] P.B. Kandagal, S.M.T. Shaikh, D.H. Manjunatha, J. Seetharamappa, B.S. Nagaralli, Spectroscopic studies on the binding of bioactive phenothiazine compounds to human serum albumin, *J. Photochem. Photobiol.* 189 (2007) 121–127, <https://doi.org/10.1016/j.jphotochem.2007.01.021>.
- [68] E. Perianu, I. Rau, L.E. Vijan, DNA influence on norfloxacin fluorescence, *J. Spectrochim. Acta A Mol. Biomol. Spectrosc.* 206 (2019) 8–15, <https://doi.org/10.1016/j.saa.2018.07.092>.
- [69] D.B. Nike, P.N. Moorthy, K.I. Priyadarsini, Nonradiative energy transfer from 7-amino coumarin dyes to thiazine dyes in methanolic solutions, *J. Chem. Phys. Lett.* 168 (1990) 533–538, [https://doi.org/10.1016/0009-2614\(90\)85666-Z](https://doi.org/10.1016/0009-2614(90)85666-Z).
- [70] M.H. Rahman, T. Maruyama, T. Okada, K. Yamasaki, M. Otagiri, Spectroscopic Study of interaction of carprofen and its enantiomers with human serum albumin-I. Mechanism of binding studied by dialysis and spectroscopic methods, *J. Biochem. Pharmacol.* 46 (1993) 1721–1731, [https://doi.org/10.1016/0006-2952\(93\)90576-1](https://doi.org/10.1016/0006-2952(93)90576-1).
- [71] L. Antonov, G. gergov, V. Petrov, M. Kubista, UV-Vis spectroscopic and chemometric study on the aggregation of ionic dyes in water, *J. Talanta* 49 (1999) 99–106, [https://doi.org/10.1016/S0039-9140\(98\)00348-8](https://doi.org/10.1016/S0039-9140(98)00348-8).
- [72] Z.C. Liu, B.D. Wang, Z.Y. Yang, Y. Li, D.D. Qin, T.R. Li, Synthesis, crystal structure DNA, interaction and antioxidant activities of two novel water-soluble Cu(2+) complexes derived from 2-oxo-quinoline-3-carbaldehyde Schiff-bases, *Eur. J. Med. Chem.* 44 (2009) 4477–4484, <https://doi.org/10.1016/j.ejmech.2009.06.009>.
- [73] B. Qiu, L. Guo, W. Wang, G. Chen, Synthesis of a novel fluorescent probe useful for DNA detection, *Biosens. Bioelectron.* 22 (2007) 2629–2635, <https://doi.org/10.1016/j.bios.2006.10.036>.
- [74] S. Satyanarayana, J.C. Dabrowiak, J.B. Chaires, Neither delta- nor lambda tris (phenanthroline) ruthenium(II) binds to DNA by classical intercalation, *Biochem.* 31 (1992) 9319–9324, <https://doi.org/10.1021/bi00154a001>.
- [75] G. Eichhorn, Y.A. Shin, Interaction of metal ions with polynucleotides and related compounds. XII. The relative effect of various metal ions on DNA helicity, *J. Am. Chem. Soc.* 90 (1968) 7323–7328, <https://doi.org/10.1021/ja01028a024>.
- [76] G.S. Senthilkumar, M. Sankarganesh, J.D. Raja, P.R.A. Jose, A. Sakthivel, T.C. Jeyakumar, R.N. Asha, Water soluble Cu(II) and Zn(II) complexes of bidentate-morpholine based ligand: synthesis, spectral, DFT calculation, biological activities and molecular docking studies, *J. Biomol. Struct. Dyn.* (2020) 1–10, <https://doi.org/10.1080/07391102.2020.1821783>.
- [77] T. Lanez, H. Benaicha, E. Lanez, M. Saidi, Electrochemical, spectroscopic and molecular docking studies of 4-methyl-5-((phenylimino)methyl)-3H- and 5-(4-fluorophenyl)-3H-1,2-dithiole-3-thione interacting with DNA, *J. Sulfur. Chem.* 39 (2018) 76–88, <https://doi.org/10.1080/17415993.2017.1391811>.